

**Supplementary materials for:**

**Functionalized dumbbell probe-based cascading exponential  
amplification DNA machine enables amplified probing of  
microRNAs**

Jie Wang<sup>a</sup>, Shuhui Li<sup>a</sup>, Jianguo Xu<sup>b\*</sup>, Yusheng Lu<sup>c</sup>, Min Lin<sup>a</sup>, Chaihong Wang<sup>a</sup>, Chen Zhang<sup>c</sup>,

Guoxing Lin<sup>a</sup>, and Lee Jia<sup>a, c\*</sup>

<sup>a</sup>Cancer Metastasis Alert and Prevention Center, and Fujian Provincial Key Laboratory of Cancer Metastasis Chemoprevention, College of Chemistry, Fuzhou University, Fuzhou 350002, China.

<sup>b</sup>School of Food and Biological Engineering, Hefei University of Technology, Hefei, 230009, China.

<sup>c</sup>Institute of Oceanography, Minjiang University, Fuzhou, Fujian 350108, China.

<sup>d</sup>School of Chemistry and Chemical Engineering, Gannan Normal University, Ganzhou 341000, P. R. China.

Correspondence should be addressed to Dr. Jianguo Xu (ORCID: <http://orcid.org/0000-0002-0187-2623>) and Dr. Lee Jia (ORCID: <http://orcid.org/0000-0001-6839-5545>).

Email: [jgxu0816@163.com](mailto:jgxu0816@163.com) or [jgxu-sfse@hfut.edu.cn](mailto:jgxu-sfse@hfut.edu.cn) (J.G. Xu)

[cmapcjia1234@163.com](mailto:cmapcjia1234@163.com) or [jjiali@fzu.edu.cn](mailto:jjiali@fzu.edu.cn) (L. Jia)

## **Experimental section**

### **Materials and reagents**

The oligonucleotides of DNA and RNA (**Table S1**) used in this study were all synthesized by Sangon Biotech Co. Ltd. (Shanghai China) and purified by HPLC. The 25-mM tris-buffer (pH 8.2) containing 10 mM MgAc<sub>2</sub>, 50 mM KAc, 100 mM NaCl, and 1 mM DTT was used as the reaction solution. The thioflavin T (ThT), dNTPs, and nucleic acids modifying enzymes of T4 DNA ligase, Klenow Fragment (3'-5'exo-) polymerase, and Nt. BbvCI endonuclease were purchased from Dingguo Changsheng Biotechnology Co., Ltd (Beijing, China). The whole blood miRNA extraction kit (HaiGene, B1803) was provided by HaiGene Biotechnology Co. Ltd. Ultrapure water obtained from a Kerton lab MINI water purification system (UK, resistance = 18 MΩ/cm) was used in all runs. All chemicals were of analytical reagent grades and used as received without further purification.

### **Instruments**

A fluorescence spectrophotometer (FL-7000, Shimadzu, Kyoto, Japan) was used to conduct the fluorescent measurements with the following settings as: excitation wavelength, 442 nm (slit= 5 nm); scanning speed, 600 nm/min; recording range, 450-600 nm; PMT detector voltage, 600V. The 10% denaturing polyacrylamide gel was performed on a DYY-6C electrophoresis analyzer (Liuyi Instrument Company, China) and imaged on a Bio-rad ChemDoc XRS (Bio-Rad, USA). The controlling of the reaction temperature is based on a TU-200 Block Heater (Yiheng Co. Ltd., Shanghai, China).

### **CEA-DNA nanomachine based miRNA-21 detection**

The CEA-DNA nanomachine based miRNA assay was conducted by firstly mixing 147  $\mu\text{L}$  of dd- $\text{H}_2\text{O}$ , 4  $\mu\text{L}$  of 10  $\mu\text{M}$  FDP, and 2  $\mu\text{L}$  of target miRNA-21 at various concentrations together. After annealed at 90  $^\circ\text{C}$  for 5 min and slowly cooled down to room temperature, the mixture was added with 20  $\mu\text{L}$  T4 DNA ligase buffer and 1  $\mu\text{L}$  of 5 U/ $\mu\text{L}$  T4 DNA ligase, and incubated at 16  $^\circ\text{C}$  for 2 h with a gentle vortex. Subsequently, 3  $\mu\text{L}$  of 10 mM dNTPs, 0.5  $\mu\text{L}$  of 5 U/ $\mu\text{L}$  Klenow Fragment (3'-5' exo-) polymerase, 10  $\mu\text{L}$  of NEB buffer 2, 0.5  $\mu\text{L}$  of 10 U/ $\mu\text{L}$  Nt. BbvCI endonuclease, and 10  $\mu\text{L}$  of Cut smart buffer were consecutively added to the above solution to induce the CEA-DNA nanomachine at 37  $^\circ\text{C}$  for 3 h. This is followed by annealing at 80  $^\circ\text{C}$  for 20 min to end the movement of the DNA nanomachine. Finally, 2  $\mu\text{L}$  of 3  $\mu\text{M}$  ThT was injected to interact with the produced G-quadruplex moieties at 37  $^\circ\text{C}$  for 1 h. The resulting solutions can be directly transformed to a cuvette for fluorescence collections.

### **MiRNA extraction**

Extraction of miRNA from whole blood was performed using the whole blood miRNA extraction kit (HaiGene, B1803, HaiGene Biotechnology Co. Ltd.) according to indicated instructions. In brief, 300  $\mu\text{L}$  of miRNA Reagent A and 150  $\mu\text{L}$  of anticoagulated whole blood (kindly provided by the Fuzhou General Hospital of Nanjing Military Command) were firstly mixed and incubated at room temperature for 5 min to fully lyse the cells. After further added with 250  $\mu\text{L}$  of miRNA Reagent B, the

mixture was centrifuged at 13,000 rpm for 5 min. The supernatant (550  $\mu$ L) was collected and added with 200  $\mu$ L of absolute ethanol. After being thoroughly mixed and incubated at room temperature for 5 min, the obtained solution was centrifuged at 13,000 rpm for 10 min to collect 700  $\mu$ L of the corresponding supernatant. This is followed by adding 300  $\mu$ L of isopropanol to the supernatant. Subsequently, the extracted miRNA in mixed solution was absorbed by the miRNA adsorption column under the condition of centrifugation at 13,000 rpm for 1 min. The interferences were successively washed away by 700  $\mu$ L of 75% isopropanol and 500  $\mu$ L of absolute ethanol, respectively. Finally, the extracted miRNAs on the absorption column were eluted by 30  $\mu$ L of Rnase Free TE buffer. The obtained miRNAs can be directly used.

### **Cell culture and RT-qPCR operation**

The human breast cancer cell line of MCF-7 and the cervical cancer cell line of HeLa were ordered from the Chinese Academy of Sciences (Shanghai), which were cultured in Dulbecco's modified Eagle's medium (supplemented with 10% FBS, 100 U/mL penicillin, and 100 mg/mL streptomycin) and grown as adherent monolayer in a humidified atmosphere containing 5% CO<sub>2</sub> at 37 °C . At their exponential growth stages, they were harvested and treated with the Trizol reagent (Invitrogen) to extract total RNAs. For implementing the RT-qPCR amplification, the PrimeScript RT reagent kit (Takara) was used according to the manufacturer's protocol and reported method<sup>1</sup>. For the transcription step, the stem-loop reverse transcription primer for miRNA-21 is: 5'-GTCGTATCCAGTGCAGGGTCCGAGGTATTCGCACTGGATACGACTCAACA

TCAGTCTGATAAGCTA-3' and a short linear reverse transcription primer for U6 RNA is : 5'-AACGCTTCACGAATTTGCGT-3'. After that, the RT-qPCR was performed by using the replication primers below: MiRNA-21 forward primer: 5'-GCCGCTAGCTTATCAGACTGATGT-3'; MiRNA-21 reverse primer: 5'-GTGCAGGGTCCGAGGT-3'; U6 RNA forward primer: 5'-CTCGCTTCGGCAGCACA-3'; U6 RNA reverse primer: 5'-AACGCTTCACGAATTTGCGT-3'.

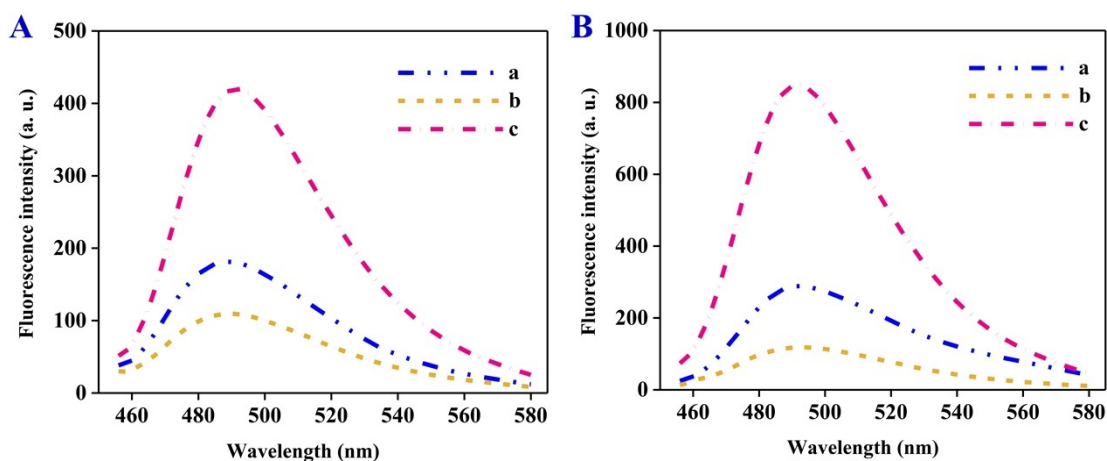


**Figure S1.** (A) Fluorescence validation of the signal reporting and amplification ability of SGQ: (a)SGQ+ThT;(b)FDP+ligase+SGQ+Polymerase+ThT;(c)FDP+ligase+SGQ+Polymerase+Nickase+ThT. (B) Fluorescence validation of the signal reporting and amplification ability of TGQ: (a) TGQ+ThT;(b)FDP+ligase+TGQ+Polymerase+ThT;(c)FDP+ligase+TGQ+Polymerase+Nickase+ThT. [SGQ]=[TGQ]=50 mM; [ThT]= 30 mM.

### Demonstration of SGQ and TGQ induced signal reporting and amplification

As is known that ThT becomes fluorescent in the presence of the G-quadruplex structure, we herein demonstrate that if the produced SCG and TGQ in our amplification system have the ability to either recognize with ThT for fluorescence reporting or complementary with sealed FDP for substantial signal enhancement. From **Figure S1A**, we can observe that the mixture of SGQ and ThT (line a) displayed a distinctive peak fluorescence at 492 nm. Interestingly, addition of polymerase into sample a cause an obvious signal improvement (line b), while addition of polymerase and nickase can induce a maximum fluorescence response (line c). These observations suggest that the SGQ itself definitely holds the reporting ability and can be extended on sealed FDP to trigger the nanomachine-like operation to amplify greatly the output

signal. **Figure S1B** was the gathered corresponding data of TGQ, which shown a same increasing change trend as that of **Figure S1A**. Therefore, the reporting ability and signal amplification ability of TGQ are confirmed.

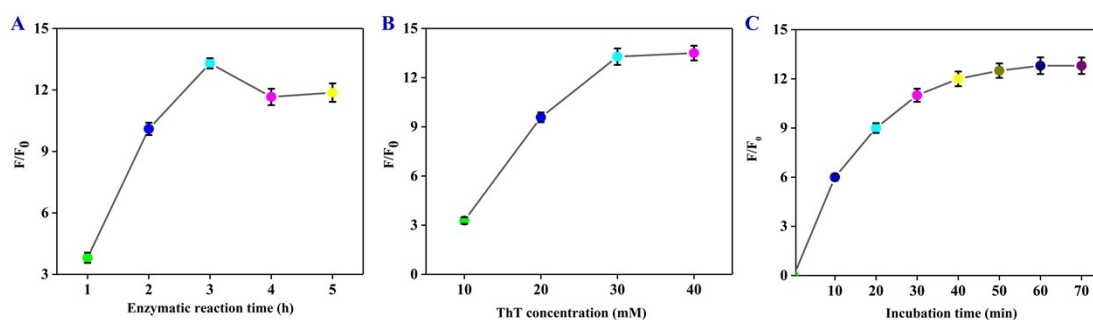


**Figure S2.** Effects of the enzymatic reaction time (A), ThT concentration (B), and the incubation time for ThT binding (C) on the assay performance.

### Optimization of experimental conditions

In order to achieve the best assay performance, the effects of the enzymatic reaction time for polymerization and nicking, the ThT concentration, and the incubation time for G-quadruplexes and ThT interaction were all carefully investigated. The value of  $F/F_0$  was adopted to evaluate the sensing ability, where  $F$  and  $F_0$  represented the peak fluorescence intensity in the presence and absence of target miRNA-21, respectively. As shown in **Figure S2A**, the highest  $F/F_0$  was obtained at 3 h. This is attributed to the fact that the signal increase of the positive sample ( $F$ ) occupies the prominent positions within 3 h. However, further increase of the enzymatic reaction, such as 4 h or 5 h, can induce inevitable background ( $F_0$ ) that comprised the  $F/F_0$  ratio. We, therefore, employ 3 h as the optimal enzymatic time for strand polymerization and nicking. Of note, the reaction time (2 h) for T4 DNA ligase based ligation was referred to the previous work<sup>2</sup>. **Figure S2B** displayed the dependence of the  $F/F_0$  on the ThT concentration. It can be found that the signal response increased with the increasing of the ThT concentration from 10 to 30 mM, and then slightly changed after further increase of the ThT concentration from 30 mM to 40 mM. This means that 30 mM of ThT is sufficient to

be bound with the generated G-quadruplexes to emit remarkable fluorescence. Thus, 30 mM of ThT was selected in the following experiments. Last, but not least, the incubation time for ThT binding was optimized in **Figure S2C**, from where we can easily observed that the  $F/F_0$  change tendency is very similar as that of **Figure S2B**. So, we chosen 1 h as the best incubation time for ThT binding for the assay.

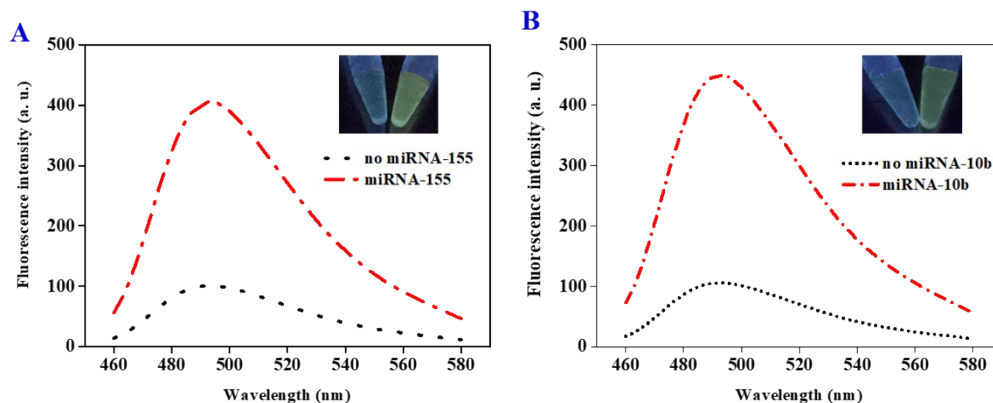


**Figure S3.** Fluorescence measurements of FDP1 and FDP2 based CEA-DNA machines in the absence and presence of miRNA-155 (A) and miRNA-10b (B), respectively. Inset provides the corresponding photography obtained under UV light. Experimental conditions: [FDP1]=[FDP2]=150 nM, [miRNA-155]=[miRNA-10b]=50 nM, and [ThT]= 30 mM.

### Universality demonstration of the CEA-DNA machine

To expand our proposed CEA-DNA machine for analyzing of other miRNAs, a couple of FDPs named as FDP1 and FDP2 were designed in **Table S1** to test miRNA-155 and miRNA-10b, respectively. As examined in **Figure S3**, the absence of miRNA-155 exhibited a weak fluorescence response of the FDP1 based CEA-DNA machine, while introduction of miRNA-155 into the FDP1 based CEA-DNA machine caused a remarkable signal enhancement. Similarly, the FDP2 based CEA-DNA machine before and after added with miRNA-10b displayed a great signal improvement. Moreover, the corresponding photography shown that the target analytes-presented samples are fluorescence-visible. All these results strongly demonstrate the feasibilities of the FDP1 and FDP2 based CEA-DNA machines. Of note, their slight differences of amplification efficiency are possibly ascribed to their different sequence designs.

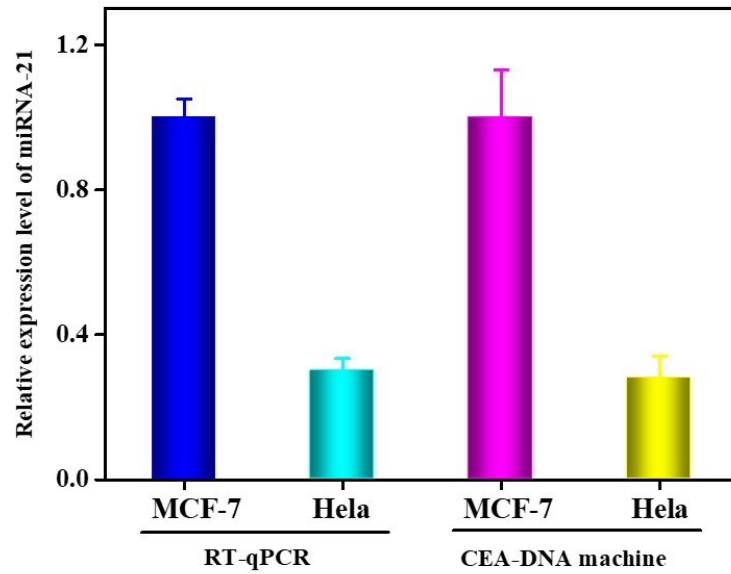


**Figure S4.** Compare relative expression levels of miRNA-21 in MCF-7 cells and HeLa cells in RT-qPCR assay and CEA-DNA assay.

#### **Comparison of RT-qPCR assay with CEA-DNA assay**

To confirm the reliability of the CEA-DNA machine, the miRNA expression level in cancer cells were simultaneously quantified by a commercial RT-qPCR kit and the current CEA-DNA machine. RT-qPCR was performed to detect miRNA-21 from MCF-7 cells and HeLa cells. Details of the RT-qPCR procedures are given in the experimental section. As can be seen in **Figure S4**, the relative expression level of miRNA-21 in MCF-7 cells and HeLa cells obtained by the CEA-DNA machine is good consistent with the RT-qPCR assay and in accordance with literature reports that the miRNA-21 in MCF-7 cells is highly expressed than HeLa cells, indicating the reliability of our proposed FDP based CEA-DNA machine.

**Table S1.** Oligonucleotides used in the current study.

Note	Sequence (5'-3')
	P-
Functionalized dumbbell probe (FDP)	<u>TCAACATCAGT</u> CTGATAAGCTCCCTAACCCCTAACCCCTgctgaggCTGATGTTGACGTCGACTCCCTAACCCCTAACCCCTGTCGACG
Functionalized dumbbell probe1 (FDP1)	P- <u>CCATCACG</u> ATTAGCATTCCCTAACCCCTAACCCCTAACCCCTgctgaggCGTGATGGGACTGTCGACTCCCTAACCCCTAACCCCTGTCGACAGTC
Functionalized dumbbell probe2 (FDP2)	P- <u>AAATTCGGT</u> TCTACAGGGCCCTAACCCCTAACCCCTAACCCCTgctgaggCCGAATTTGACTGTCGACTCCCTAACCCCTAACCCCTGTCGACAGTC
Single G-quadruplex (SGQ)	TCAGCAGGGTTAGGGTTAGGGTTAGGGAGCTTATCAGACTGATGTTGA
Twin G-quadruplex (TGQ)	TCAGCAGGGTTAGGGTTAGGGTTAGGGAGCTTATCAGACTGATGTTGACGTCGACAGGGTTAGGGTTAGGGTTAGGGTTAGGGAGTTCGACGTCAACATCAGCC
Target (miRNA-21)	<u>UAGCUUAUCAGACUGAUGUUGA</u>
miRNA-155 (miRNA-155)	UUAAUGCUAAUCGUGAUGGGG
miRNA-125b (miRNA-125b)	UCCCUGAGACCCUAACUUGUGA
miRNA-145 (miRNA-145)	GUCCAGUUUCCCAGGAAUCCCTU
miRNA-10b (miRNA-10b)	UACCCUGUAGAACCGAAUUUGU

For FDP, the underlined region (Region I) is the complementary region of target miRNA-21 stimulus. The seven bases shown in lowercase letters (Region II) is the half recognition site of Nt. BbvCI. The two grey shadowed fragments (Region III) riched with “C” bases are the complementary sequences of G-quadruplex for producing SGQ and TGQ. In addition, its 5’ end and 3’ end are phosphorylated and exposed, respectively. They can be forced to the adjacent positions through the hybridization of two red-colored domains (stem I) and two blue-colored domains (stem II). FDP1 and FDP2 are identical designed as that of FDP to specifically recognize miRNA-155 and miRNA-10b, respectively. The SGQ and TGQ are synthesized to have the same base sequence as the product of the 1<sup>st</sup> DNA nanomachine and 2<sup>nd</sup> DNA nanomachine, respectively. The non-targets of miRNA-155, miRNA-125b, miRNA-145, and miRNA-10b are randomly selected against miRNA-21.



**Table S2.** Overview of the assay performance comparison of the CEA-DNA nanomachine with other optical or electrochemical sensors for nucleic acids detection.

<b>Method</b>	<b>LOD</b>	<b>Linear range</b>	<b>Orders of amplitude</b>	<b>Category</b>	<b>Ref.</b>
Fluorescence quenching of positively charged gold nanoparticles to silver nanoclusters	33.4 fM	100 fM-1.0 nM	5	Fluorescent assay	3
Gold-nanorod functionalized polydiacetylene microtube waveguide	0.01 nM	0.05 nM-1 nM	2	Fluorescent assay	4
Toehold-mediated strand displacement reaction and DNA tetrahedron substrate	5 fM	0.05 pM-1 pM	2	Fluorescent assay	5
Zinc finger protein specific to DNA-RNA hybrids	2 fM	2 fM-1 nM	7	Electrochemical assay	6
Colorimetric PCR-based amplification	5 fM	5 fM- 50 pM	5	Colorimetric assay	7
Triple signal amplification	3 fM	10 fM-5 pM	3	Electrochemical assay	8
CEA-DNA nanomachine	0.1 fM	0.1 fM-1 nM	8	Fluorescent assay	Current study

**Table S3.** Recoveries from miRNA-21 spiked human serum samples (1% and 5%)

Sample	Spiked (fM)	Found (fM)	Recovery (%)	RSD (%)
1% Human serum	1	0.948	94.8	1.15
	2	97.5	97.5	2.3
	3	10130	101.3	1.23
5% Human serum	1	0.982	98.2	1.74
	2	94.6	94.6	3.22
	3	9336	93.4	2.35

The recovery of the CEA-DNA nanomachine was examined by analyzing the spiked samples of 1 fM, 100 fM, and 10 pM concentrations of miRNA-21 with the presence of 1% human serum and 5% human serum, respectively. **Table S3** displayed that even the miRNA-21 was at very low concentrations, they can be accurately determined with a desirable recovery rates in the range from 94.8% to 101.3% and 93.4% to 98.2%, respectively, convincing further its application prospects for real samples. As many hydrolases and proteins are presently in the human serum, the recovery rate also proven that the CEA-DNA nanomachine has a much stronger anti-serum interference ability.

## References

1. J. Xu, Z.-S. Wu, Z. Wang, J. Le, T. Zheng and L. Jia, *Biomaterials*, 2017, **120**, 57-65.
2. J. Wang, H.-y. Dong, Y. Zhou, L.-y. Han, T. Zhang, M. Lin, C. Wang, H. Xu, Z.-S. Wu and L. Jia, *Biosensors and Bioelectronics*, 2018, **122**, 239-246.
3. X. Miao, Z. Cheng, H. Ma, Z. Li, N. Xue and P. Wang, *Analytical chemistry*, 2018, **90**, 1098-1103.
4. Y. Zhu, D. Qiu, G. Yang, M. Wang, Q. Zhang, P. Wang, H. Ming, D. Zhang, Y. Yu, G. Zou, R. Badugu and J. R. Lakowicz, *Biosensors & bioelectronics*, 2016, **85**, 198-204.
5. W. Li, W. Jiang, Y. Ding and L. Wang, *Biosensors & bioelectronics*, 2015, **71**, 401-406.
6. C. S. Fang, K. S. Kim, B. Yu, S. Jon, M. S. Kim and H. Yang, *Analytical chemistry*, 2017, **89**, 2024-2031.
7. J. Dong, G. Chen, W. Wang, X. Huang, H. Peng, Q. Pu, F. Du, X. Cui, Y. Deng and Z. Tang, *Analytical chemistry*, 2018, **90**, 7107-7111.
8. L. Liu, N. Xia, H. Liu, X. Kang, X. Liu, C. Xue and X. He, *Biosensors & bioelectronics*, 2014, **53**, 399-405.